Journal of Coordination Chemistry

ISSN: 0095-8972 (Print) 1029-0389 (Online) Journal homepage: http://www.tandfonline.com/loi/gcoo20

[Ni(bpy)(ox)]: a candidate in the class of Haldane gap systems (bpy = 2,2′-bipyridine, ox = oxalate)

J. Černák, N. Farkašová, M. Tomás, V. Kavečanský, E. Čižmár & M. Orendáč

To cite this article: J. Černák, N. Farkašová, M. Tomás, V. Kavečanský, E. Čižmár & M. Orendáč (2015) [Ni(bpy)(ox)]: a candidate in the class of Haldane gap systems (bpy = 2,2#-bipyridine, ox = oxalate), Journal of Coordination Chemistry, 68:16, 2788-2797, DOI: 10.1080/00958972.2015.1058485

To link to this article: http://dx.doi.org/10.1080/00958972.2015.1058485

Accepted author version posted online: 05 Jun 2015.
Published online: 09 Jul 2015.

Journal of Coordination Chemistry, 2015
Vol. 68, No. 16, 2788–2797, http://dx.doi.org/10.1080/00958972.2015.1058485

[Ni(*bpy*)(*ox*)]: a candidate in the class of Haldane gap systems (*bpy* = 2,2′-bipyridine, *ox* = oxalate)

J. ČERNÁK*†, N. FARKAŠOVÁ†, M. TOMÁS‡, V. KAVEČANSKÝ§, E. ČIŽMÁR¶ and M. ORENDÁČ¶

†Department of Inorganic Chemistry, Institute of Chemistry, Faculty of Sciences, P.J. Šafárik University in Košice, Košice, Slovakia
‡Departamento de Química Inorgánica, Instituto de Sintesis Química y Catálisis Homogénea (ISQCH), CSIC-University of Zaragoza, Zaragoza, Spain
§Slovak Academy of Sciences, Institute of Experimental Physics, Košice, Slovakia
¶Institute of Physics, Faculty of Sciences, P.J. Šafárik University in Košice, Košice, Slovakia

(*Received 1 February 2015; accepted 19 May 2015*)

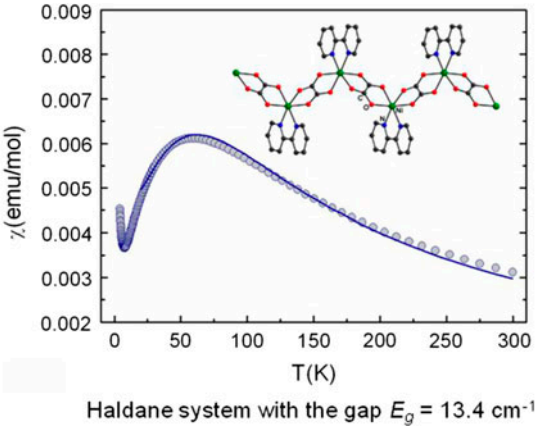

[Ni(*bpy*)(*ox*)] (*bpy* = 2,2′-bipyridine; *ox* = oxalate) was solvothermally prepared in the microcrystalline form and identified by chemical analyses and IR spectroscopy. X-ray powder diffractometry indicates its isostructural character with analogous complexes [M(*bpy*)(*ox*)], and thus, its chain-like crystal structure formed of {Ni(*bpy*)} building units linked by bridging oxalate anions coordinated in a bis(chelate) fashion. The temperature dependence of the magnetic susceptibility and the field dependence of the magnetization reveal that the studied compound belongs to the class of systems with a Haldane gap. The estimated magnitude of the gap $E_g \approx 13.4$ cm^{-1} is comparable with those found in archetypal Haldane gap systems.

Keywords: Nickel; Oxalate; 2,2′-Bipyridine; Chain structure; Rietveld method; Haldane gap; Excitation spectrum; Quantum spin chain

*Corresponding author. Email: juraj.cernak@upjs.sk.

1. Introduction

Due to a variety of coordination modes, the oxalate dianion (*ox*, $C_2O_4^{2-}$) has been a useful bridging species in synthetic design of oligomeric and polymeric systems with different topologies [1–8]. In addition, oxalate is an efficient mediator of magnetic exchange interactions [1, 3, 9, 10]. Exploring the rigid symmetric bis-chelate coordination mode of *ox* resulted in many one-dimensional (1-D) complexes based on Ni(II) [5, 10–16], which were shown to be representative of Haldane gap or spin glass behavior [17–19]. The Haldane conjecture about fundamentally different behavior of quantum spin with integer and half-integer spins is well established, but compounds in which the Haldane gap is found are still intensively investigated. The current interest is mainly stimulated by theoretically predicted quantum phase transition between Haldane phase and large-D phase [20]. Consequently, the effort is devoted to the syntheses of $S = 1$ Heisenberg antiferromagnetic chains with appropriate values of exchange coupling and single-ion anisotropy.

Previously, as part of our broader study of structures and/or magnetic behavior of 1-D systems we synthesized, structurally characterized and studied the magnetic properties of several Ni(II) ($S = 1$) compounds exhibiting chain-like structures, in which the paramagnetic Ni(II) ions were linked by bridging cyanidocomplex anions [21]. The use of cyanidocomplex anion as a linker in these compounds led to a large separation of the paramagnetic Ni(II) ions via the long diamagnetic {–N≡C–M–C≡N–} bridge (about 10 Å) and, as a consequence, the observed magnetic exchange interactions were weak [22–24]. In order to shorten the Ni(II)···Ni(II) separation between paramagnetic Ni(II) ions, we decided to replace the cyanidocomplex anion by oxalate. As a result of our synthetic experiments, we have prepared [Ni(*bpy*)(*ox*)] (**1**) (*bpy* = 2,2′-bipyridine). Analogous compounds [M(*bpy*)(*ox*)] (M = Co, Mn, Cu, Fe, Zn) were already structurally characterized and are isostructural [6, 25–30]. Here, we report the synthesis, spectroscopic, structural and magnetic characterization of **1** which is a member of the Haldane gap system class.

2. Experimental

2.1. *Materials*

$NiC_2O_4{\cdot}2H_2O$, 2,2′-bipyridine and ethanol were purchased from commercial sources and used as received.

2.2. *Synthesis*

Teflon lined autoclave (25 mL) was filled with water (5 cm^3), ethanol (5 cm^3), solid $NiC_2O_4{\cdot}2H_2O$ (0.0914 g, 0.5 mmol) and solid 2,2′-bipyridine (0.0781 g, 0.5 mmol). The formed reaction mixture was heated from 298 to 433 K in 2 h and maintained at 433 K for 30 h. After the mixture was cooled to room temperature in 40 h, the formed blue microcrystalline powder of **1** was isolated, washed with a small volume of water and dried in air. Yield: 76% (0.115 g). Anal. Calcd. for $C_{12}H_8N_2NiO_4$ ($M = 302.90$ g M^{-1}) (%): C, 47.58; H, 2.66; N, 9.25. Found: C, 46.91; H, 2.59; N, 8.87. IR (cm^{-1}): 3098 w, 3085 w, 3072 w, 3051 w, 3030 w, 1674 s, 1599 vs, 1564 m, 1491 w, 1473 w, 1445 m, 1417 sh, 1358 m, 1316 m, 1308 m, 1253 w, 1227 m, 1176 w, 1017 w, 979 w, 913 w, 801 m, 777 m, 767 s, 749 w, 736 m, 654 w, 634 w, 552 w, 524 w, 485 m, 433 w, 421 m, 414 m.

2.3. *Physical measurements*

Elemental analysis was performed on a CHNOS Elemental Analyzer vario MICRO (Elementar Analysensysteme GmbH). Infrared spectra were recorded on a Nicolet 6700 FT-IR spectrophotometer (Thermo Scientific) equipped with a diamond crystal Smart Orbit^{TM} from 4000 to 400 cm^{-1}.

X-ray powder diffraction investigation of the crystal structure was performed by an Ultima IV (Rigaku) powder diffractometer in semifocusing (Bragg-Brentano) geometry using CuK_α radiation, detected by a 1-D semiconductor detector D/teX Ultra. The preliminary data processing, phase identification and finally the Rietveld refinement of the crystal structure were performed using PDXL2 Rigaku software package [31]. The unit cell dimensions were corrected with respect to the external standard LaB_6 (NIST 660b).

2.4. *Magnetic measurements*

The temperature dependence of magnetic susceptibility and the field dependence of magnetization were investigated in a commercial SQUID magnetometer manufactured by Quantum Design. The powdered sample of 39.4 mg was located in a plastic gelcap, which was held by a straw. Magnetic field of magnitude 1 kOe was applied for susceptibility measurements. The contribution of an empty gelcap to the total signal has been subtracted from the obtained experimental data.

3. Results and discussion

3.1. *Synthesis and identification*

Blue microcrystalline **1** was prepared under solvothermal conditions using $NiC_2O_4{\cdot}2H_2O$ and *bpy* as starting materials. The chemical composition of **1** was corroborated by chemical analyses. Our attempts to prepare **1** by direct precipitation of $NiCl_2$ with oxalic acid and *bpy* in aqueous–ethanolic solution led to the same product as indicated by IR spectroscopy, but with low crystallinity not suitable for the powder diffraction study; we assume the solvothermal conditions are more favorable for growth of larger crystallites. In order to slow the crystallization and thus to avoid the immediate precipitation of **1**, several types of diffusion experiments were carried out, but these, up to now, failed to give single crystals suitable for X-ray study.

The measured IR spectrum of **1** (figure 1) clearly indicated the presence of *bpy* and oxalate in the formed product; the observed absorption bands were identified using literature data [32–34]. Several weak absorption bands from $\nu(C_{ar}–H)$ valence stretching vibrations were observed at 3098–3051 cm^{-1}, and sharp bands from 1599 to 1417 cm^{-1} were assigned to $\nu(C_{ar}–C_{ar})$ and $\nu(C_{ar}–N)$ stretches. Bands of strong to medium intensities between 777 and 736 cm^{-1} were assigned to out of plane $C_{ar}–H$ vibrations. A characteristic absorption at 1674 cm^{-1} was assigned to $\nu_{asym}(COO^-)$ vibrations, indicating the presence of oxalate while the corresponding absorption bands of medium intensities assigned to symmetric $\nu_{sym}(COO^-)$ vibrations can be observed at 1358–1308 cm^{-1}. The absorption band at 801 cm^{-1} could be identified easily; according to the literature data, it corresponds to δ(OCO) vibrations [34, 35].

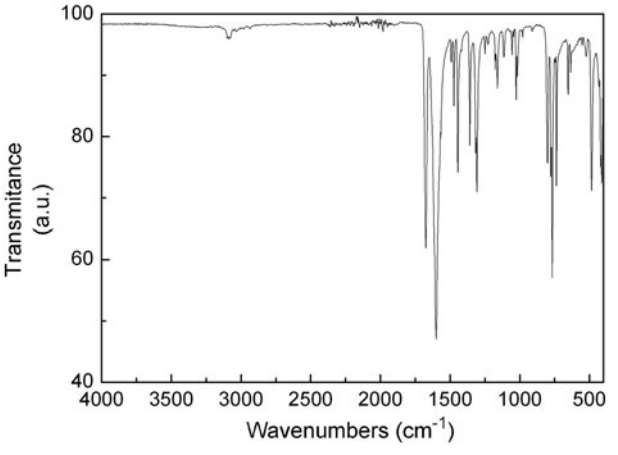

Figure 1. Infrared spectrum of **1**.

3.2. *Structure of 1*

As our efforts to prepare single crystals of **1** were unsuccessful, the microcrystalline sample of **1** was studied by powder X-ray diffraction. As can be seen from figure 2, it was possible to reproduce the experimentally obtained X-ray powder diffraction pattern assuming isostructural character of **1** with the analogous Co(II) complex [Co(*bpy*)(*ox*)] (**2**) [6, 25]. The cell parameters of **1** were refined using the fitting procedure incorporated in the Rigaku PDXL2 software and are close to that of analogous complexes [M(*bpy*)(*ox*)] (table 1). It can be seen from table 1 that the increase of the unit cell volumes of isostructural compounds [M(*bpy*)(*ox*)] correlate well with the increase of the Shannon ionic radii of the

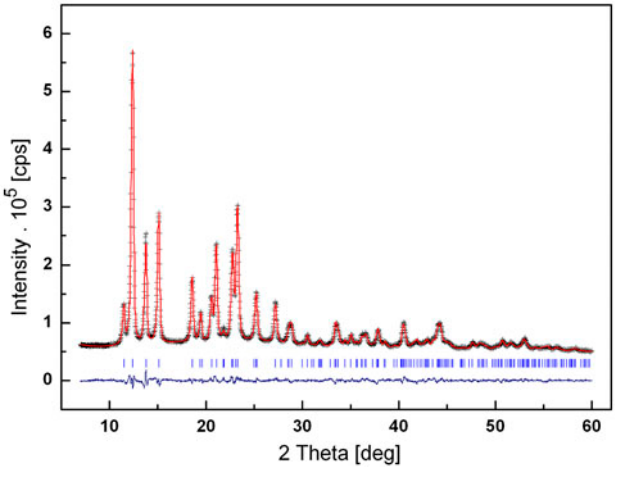

Figure 2. The Rietveld refinement plot of [Ni(*bpy*)(*ox*)]. The measured points are indicated by "+" signs while the calculated ones by the line overlaying them. The positions of all possible Bragg reflections are shown by the vertical marks in the middle. The lower curve shows the difference between the observed and calculated intensities.

Table 1. Comparison of the cell parameters [Å] of **1** and some isostructural complexes [M(*bpy*)(*ox*)].

Crystal system/space group/temperature	[Ni(*bpy*)(*ox*)] (**1**) Orthorhombic $Pna2_1$ 293 K	[Co(*bpy*)(*ox*)] (**2**) [6] Orthorhombic $Pna2_1$ 293 K	[Co(*bpy*)(*ox*)] (**2**) [25] Orthorhombic $Pna2_1$ 293 K	[Mn(*bpy*)(*ox*)] [26] Orthorhombic $Pna2_1$ 293 K	[Mn(*bpy*)(*ox*)] [27] Orthorhombic $Pna2_1$ 293 K
a (Å)	9.0406(4)	9.1275(8)	9.2333(18)	9.6475(6)	9.674(2)
b (Å)	9.1110(5)	9.2323(8)	9.2163(18)	9.2578(6)	9.2890(2)
c (Å)	14.2390(4)	14.1929(12)	14.101(3)	13.8697(9)	13.921(3)
V (Å^3)	1172.86(9)	1196.00(18)	1199.9 (4)	1238.8(1)	1250.9(4)

respective central ions Ni(II), Co(II) and Mn(II) [36]. Due to a large number of positional and thermal parameters in the structure (76 positional and isotropic thermal parameters for 19 "non-hydrogen" atoms), only the positional parameters of the NiO_4N_2 chromophore were refined. Using these parameters directly from the Co(II) complex, **2**, good agreement was obtained between the experimental and calculated profile of the powder diffraction pattern (R_{wp} = 2.58%, χ^2 = 3.14).

The obtained results of the X-ray powder diffraction allow us to suggest that **1** exhibits the same chain-like structure as in **2** in which six-coordinate Ni(II) ions (cis-O_4N_2 donor set) are linked by bis-chelate bridging oxalato ligands, and the remaining two coordination sites are occupied by chelate-bonded *bpy* (figure 3). Similar chain-like structures based on Ni(II) ions were observed in the analogous [Ni(*dpya*)(*ox*)] with 2,2′-dipyridylamine (*dpya*) used as a blocking ligand instead of *bpy* [13] or in [Ni(*en*)(*ox*)] with ethane-1,2-diamine (*en*) as a blocking ligand [10]. The 1-D crystal structures of both trans-[Ni$(H_2O)_2$(*ox*)] (linear chain) [11] and cis-[Ni$(H_2O)_2$(*ox*)] (zigzag chain) [12] were reported. As a consequence of the relatively short bis-chelating oxalate bridging, neighboring Ni(II) ions within the chain in **1** are much closer (5.380(7) Å) than in Ni$(en)_2Ni(CN)_4$ in which the paramagnetic Ni(II) ions are linked by long cyanidocomplex bridging (9.940(2) Å) [37].

The experimental Ni–O and Ni–N distances in **1** are 2.077(6)–2.109(14) and 2.094(20)–2.239(19) Å, respectively. Taking into account the limitations of the Rietveld method, the obtained values are in an acceptable range; in a similar [Ni$(bpy)_2$(*ox*)]·$5H_2O$, the Ni–N and Ni–O bonds are 2.0720(13)–2.1001(13) and 2.0359(11)–2.0673(12) Å, respectively [38].

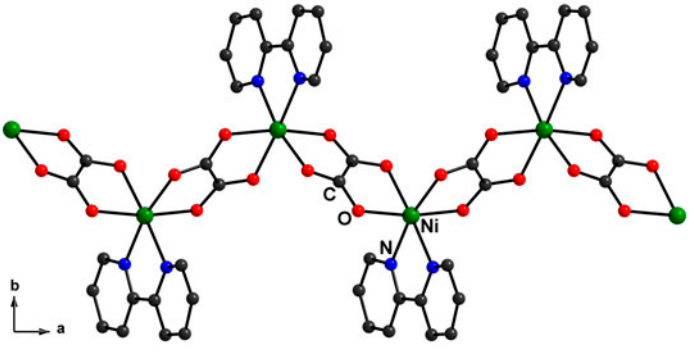

Figure 3. Schematic view of the crystal structure of **1**.

3.3. *Magnetic properties*

The magnetic susceptibility was investigated from 4.2 to 300 K, and the results are presented in figure 4. The data are characterized by a maximum located at 60 K followed by a sudden drop of susceptibility at lower temperatures. However, below 8 K, the susceptibility increases again when the temperature is decreased. Considering the aforementioned features of the susceptibility, the data above 20 K were analyzed using the prediction for $S = 1$ Heisenberg antiferromagnetic chain as proposed by Kahn *et al.* [39]. Reasonable agreement was obtained for the magnitude of exchange interaction $J = -32.6\ \mathrm{cm}^{-1}$ and g factor $g = 2.11$. The obtained value of J suggests the magnitude of Haldane gap $E_g = 0.41\ |J| = 13.4\ \mathrm{cm}^{-1}$. Similar magnitude $10.1\ \mathrm{cm}^{-1}$ of the Haldane gap was observed in an $\mu_{1,3}$-azido bridged Ni(II) complex trans-$\{(N_3)[Ni(meso\text{-}cth)]\}_n(ClO_4)_n$ (*meso-cth* = *meso* isomer of 5,7,7,12,14,14-hexamethyl-1,4,8,11-tetraazacyclotetradecane) with trans-N_4N_2 donor set and Ni···Ni distance of 6.069(4) Å [19].

The deviation between the prediction and the data occurring at lower temperatures represents the intrinsic feature of the model. Subsequent analysis was concentrated at temperature below 20 K, where two contributions were considered. The sudden drop of susceptibility with decreasing temperature, which is fully consistent with Haldane conjecture about the energy gap between the non-magnetic ground state and magnetic excited states, was analyzed using the prediction [40]:

$$\chi(T) \approx \frac{1}{\sqrt{T}} \exp\left(-\frac{E_g}{T}\right)$$

which holds for $T < E_g$. In contrast, the increase of susceptibility at lowest temperature was fitted by Curie law, $\chi(T) = xC/T$, where C represents Curie constant and x the concentration of free spins. Adopting the value of the Haldane gap $E_g = 13.4\ \mathrm{cm}^{-1}$, as obtained from the analysis of high-temperature susceptibility data, very good agreement was obtained for $x = 0.019$ and $S = 1/2$ or $x = 0.016$ and $S = 1$ free spins, respectively (figure 5). As anticipated, for temperatures higher than 15 K, the deviation between the data and the prediction starts to increase. It should be stressed that for spin chains of finite length, in which Haldane gap is present, $S = 1/2$ states are formed at the end of each segment [41]. On the

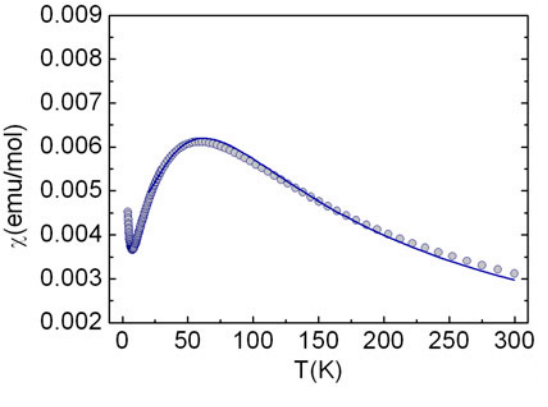

Figure 4. Temperature dependence of magnetic susceptibility in the whole temperature range. Experimental data are denoted by balls, whereas the solid line represents theoretical prediction.

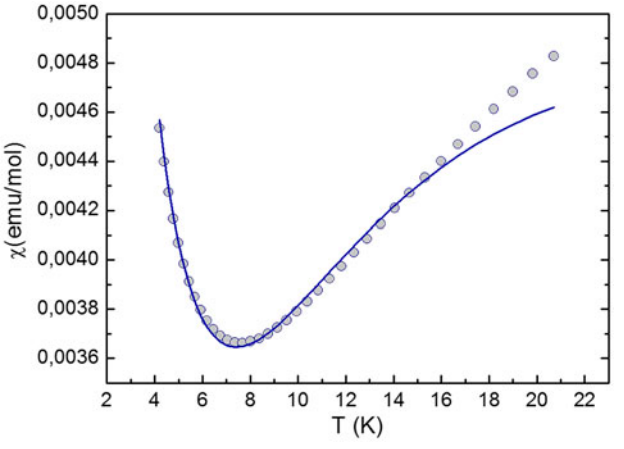

Figure 5. Temperature dependence of magnetic susceptibility at low temperatures. Experimental data are denoted by balls, whereas the solid line represents theoretical prediction. See text for a more detailed discussion.

other hand, free $S = 1$ spins may be present due to Ni(II) ions not built in chains. Considering the anticipated length of chain segments and powder nature of the sample both values of x's are acceptable. However, the powder nature of the sample does not enable to separate the two contributions, as systematic study of the influence of end chain effects ultimately requires single crystals [42].

Knowledge of the temperature dependence of susceptibility enables study of effective magnetic moment μ_{eff}, as presented in figure 6. The value of $\mu_{\text{eff}} \approx 2.75\mu_{\text{B}}$ at room temperature is somewhat smaller than the theoretical spin-only value $2.828\mu_{\text{B}}$ of free high-spin Ni (II) ions. The difference may be attributed to rather strong antiferromagnetic exchange interaction. The effective magnetic moment gradually decreases with decreasing temperature to $0.35\mu_{\text{B}}$ at 4.2 K. Such a pronounced decrease agrees with the non-magnetic ground state formed in Haldane gap systems.

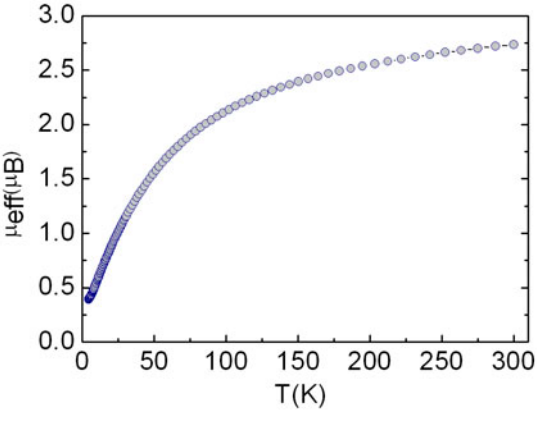

Figure 6. Temperature dependence of the effective magnetic moment.

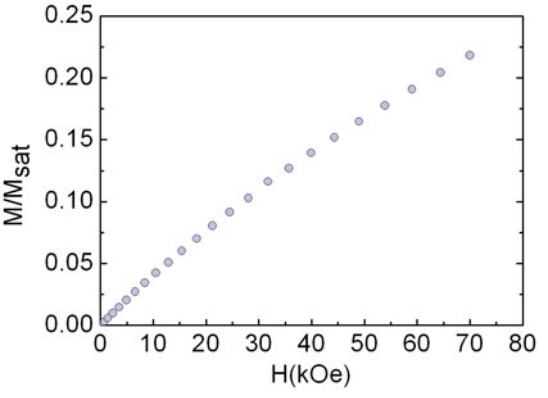

Figure 7. Magnetic field dependence of magnetization.

The physical nature of the ground state is also well demonstrated by the field dependence of magnetization. This study was performed at 5 K up to 70 kOe, and the results are presented in figure 7. As can be seen, the magnetization grows only slowly with increasing magnetic field reaching only about 20% of the saturation magnetization $M_{sat} = N_A g \mu_B S$ at $B = 70$ kOe. The small rounding may be attributed to the presence of $S = 1$ and/or $S = 1/2$ free spins as discussed above. The observed behavior strongly supports the non-magnetic ground state within the chains. Since the magnetization was studied at 5 K and $E_g = 13.4\ cm^{-1}$ (≈19.3 K), the occupation of the excited magnetic states is low. More specifically, the occupation factor $\exp(-E_g/T) \approx 0.018$ in zero magnetic field is found when the value of E_g obtained from the analysis of high-temperature susceptibility data is considered. It should be noted that if the magnetic field exceeds the value of the critical magnetic field B_c, Haldane gap is closed and the ground state becomes magnetic due to crossing of one component of the first excited triplet with the ground state level. Magnitude of $B_c \approx 145$ kOe is estimated for the studied system considering the relation $g\mu_B B_c = E_g$ [43]. Consequently, for magnetic fields up to 70 kOe, the ground state should remain non-magnetic in accord with the experimental observation. Similar behavior was observed in other Haldane gap systems, $[Ni(en)_2NO_2]BF_4$ and $[(CH_3)_4N]Ni(NO_2)_3$, where below B_c, linear-like magnetic field dependence of the magnetization was observed with the slope depending on the direction of the magnetic field [44] and temperature [45], respectively. However, the slope may also be affected by single-ion anisotropy which effectively decreases the magnitude of the Haldane gap.

Crystal field effects were neglected in the presented analysis. It is just the ratio of the single-ion anisotropy and exchange coupling constants which determines the accurate position of a system in the Haldane phase. However, accurate determination of single-ion anisotropy adopting spectroscopic techniques requires sufficiently large single crystals, which are currently not available. Nevertheless, effort in this direction is in progress.

4. Summary

Using solvothermal conditions, microcrystalline sample of [Ni(*bpy*)(*ox*)] (**1**) was isolated. Chemical analyses and IR spectroscopy corroborated its chemical identity and purity.

Powder diffraction study using Rietveld methods indicates it is isostructural with the series [M(*bpy*)(*ox*)], with M being other 3d metals, and thus, its chain-like crystal structure formed by {M(*bpy*)} structural units linked by oxalate bridges with oxalato ligands coordinated in a bis-chelate fashion. The investigation of magnetic properties of **1** strongly supports non-magnetic ground state separated from magnetic excited states by an energy gap. Such an energy spectrum in an $S = 1$ Heisenberg antiferromagnet is consistent with Haldane conjecture and, consequently, **1** can be considered as a new candidate in the class of Haldane gap systems.

Acknowledgment

NF thanks National Scholarship Programme of the Slovak Republic for financial support of her research stay at the University of Zaragoza (Spain).

Disclosure statement

No potential conflict of interest was reported by the authors.

Funding

This work was supported by the Slovak grant agencies VEGA [grant number 1/0075/13]; APVV [grant number APVV-0132-11]; VVGS [grant number VVGS-2014-164]; Ministry of Science and Innovation (Spain) [grant number MAT2011–27233-C02–01]- European Union Regional Development Fund; Diputación General de Aragón [grant number E-16]; the European Union Regional Development Fund (Slovakia) [ITMS: 26220120047].

References

[1] M. Clemente-León, E. Coronado, C. Martí-Gastaldo, F.M. Romero. *Chem. Soc. Rev.*, **40**, 473 (2011).
[2] F.A. Mautner, F.R. Louka, S.S. Massoud. *J. Mol. Struct.*, **921**, 333 (2009).
[3] Z. Smékal, Z. Trávníček, F. Lloret, J. Marek. *Polyhedron*, **18**, 2787 (1999).
[4] U. García-Couceiro, O. Castillo, A. Luque, J.P. García-Terán, G. Beobide, P. Román. *Eur. J. Inorg. Chem.*, 4280 (2005).
[5] J. Chun, Y. Lee, S. Pyo, C. Im, S.-J. Kim, H. Yum, J. Do. *Bull. Korean Chem. Soc.*, **30**, 1603 (2009).
[6] Y. Chang, K.-L. Zhang, S.-W. Ng. *Acta Cryst.*, **E65**, m1243 (2009).
[7] F.R. Fortea-Pérez, J. Vallejo, M. Inclán, M. Déniz, J. Pasán, E. García-España, M. Julve. *J. Coord. Chem.*, **66**, 3349 (2013).
[8] L.-Q. Li, M. Li, H. Zhang, S. Li, F.-M. Nie. *J. Coord. Chem.*, **67**, 847 (2014).
[9] T.D. Keene, H.R. Ogilvie, M.B. Hursthouse, D.J. Price. *Eur. J. Inorg. Chem.*, 1007 (2004).
[10] T.D. Keene, M.B. Hursthouse, D.J. Price. *Cryst. Growth Des.*, **9**, 2604 (2009).
[11] R. Deyrieux, C. Berro, A. Peneloux. *Bull. Soc. Chim. Fr.*, **1**, 25 (1973).
[12] V. Paredes-García, I. Rojas, D. Venegas-Yazigi, E. Spodine, J.A.L.C. Resende, M.G.F. Vaz, M.A. Novak. *Polyhedron*, **30**, 3171 (2011).
[13] J.Y. Lu, T.J. Schroeder, A.M. Babb, M. Olmstead. *Polyhedron*, **20**, 2445 (2001).
[14] O. Castillo, A. Luque, P. Román, F. Lloret, M. Julve. *Inorg. Chem.*, **40**, 5526 (2001).
[15] O. Castillo, A. Luque, F. Lloret, P. Román. *Inorg. Chim. Acta*, **324**, 141 (2001).
[16] J.H. Guo. *Acta Cryst.*, **E67**, m1832 (2011).
[17] C.P. Landee, K.A. Reza, M.R. Bond, R.D. Willett. *Phys. Rev. B*, **56**, 147 (1997).
[18] M. Yamashita, T. Ishii, H. Matsuzaka. *Coord. Chem. Rev.*, **198**, 347 (2000).
[19] M. Salah El Fallah, A. Escuer, R. Vicente, X. Solans, M. Font-Bardia, M. Verdaguer. *J. Cryst. Growth*, **344**, 133 (2011).
[20] K. Wierschem, P. Sengupta. *Phys. Rev. Lett.*, **112**, 247203 (2014).

[21] J. Černák, M. Orendáč, I. Potočňák, J. Chomič, A. Orendáčová, J. Skoršepa, A. Feher. *Coord. Chem. Rev.*, **224**, 55 (2002).
[22] J. Černák, J. Lipkowski, E. Čižmár, A. Orendáčová, M. Orendáč, A. Feher, M.W. Meisel. *Solid State Sci.*, **5**, 579 (2003).
[23] J. Černák, K.A. Abboud, J. Chomič, M.W. Meisel, M. Orendáč, A. Orendáčová, A. Feher. *Inorg. Chim. Acta*, **311**, 126 (2000).
[24] M. Orendáč, A. Orendáčová, J. Černák, A. Feher, P.J.C. Signore, M.W. Meisel, S. Merah, M. Verdaguer. *Phys. Rev.*, **B52**, 3435 (1995).
[25] P.-Z. Li, Q. Xu. *Acta Cryst.*, **E65**, m508 (2009).
[26] D. Deguenon, G. Bernardinelli, J.-P. Tuchagues, P. Castan. *Inorg. Chem.*, **29**, 3031 (1990).
[27] J.-H. Yu, Q. Hou, M.-H. Bi, Z.-L. Lü, X. Zhang, X.-J. Qu, J. Lu, J.-Q. Xu. *J. Mol. Struct.*, **800**, 69 (2006).
[28] J. Luo, M. Hong, Y.C. Liang, R. Cao. *Acta Cryst.*, **E57**, m361 (2001).
[29] H.-K. Fun, S.S. Raj, X. Fang, L.-M. Zheng, X.-Q. Xin. *Acta Cryst.*, **C55**, 903 (1999).
[30] X.-R. Lin, B.-Z. Ye, J.-S. Liu, C.-X. Wei, J.-X. Chen. *Acta Cryst.*, **E62**, m2130 (2006).
[31] *Rigaku J.*, **26**, 23–27 (2010).
[32] J.S. Strukl, J.L. Walter. *Spectrochim. Acta Part A*, **27**, 209 (1971).
[33] J.S. Strukl, J.L. Walter. *Spectrochim. Acta Part A*, **27**, 223 (1971).
[34] O. Castillo, A. Luque, S. Iglesias, C. Guzmán-Miralles, P. Román. *Inorg. Chem. Commun.*, **4**, 640 (2001).
[35] M.L. Calatayud, I. Castro, J. Sletten, F. Lloret, M. Julve. *Inorg. Chim. Acta*, **300–302**, 846 (2000).
[36] R. Shannon, C.T. Prewitt. *Acta Crystallogr. Sect. B Struct. Crystallogr. Cryst. Chem.*, **B25**, 925 (1969).
[37] J. Černák, J. Chomič, D. Baloghová, M. Dunaj-Jurčo. *Acta Cryst.*, **C44**, 1902 (1988).
[38] N. Farkašová, J. Černák, M. Tomás, L.R. Falvello. *Acta Cryst.*, **C70**, 477 (2014).
[39] A. Meyer, A. Gleizes, J.-J. Girerd, M. Verdaguer, O. Kahn. *Inorg. Chem.*, **21**, 1729 (1982).
[40] D. Coombes, T. Xiang, G.A. Gehring. *J. Phys.: Condens. Matter*, **10**, L159 (1998).
[41] A. Lappas, V. Alexandrakis, J. Giapintzakis, V. Pomjakushin, K. Prassides, A. Schneck. *Phys. Rev.*, **B66**, 144281 (2002).
[42] G.E. Granroth, S. Maegawa, M.W. Meisel, J. Krzystek, L.-C. Brunel, N.S. Bell, J.H. Adair, B.H. Ward, G.E. Fanucci, L.-K. Chou, D.R. Talham. *Phys. Rev.*, **B58**, 9312 (1998).
[43] Ch.P. Landee, M.M. Turnbull. *J. Coord. Chem.*, **67**, 375 (2014).
[44] V.C. Long, Y.-H. Chou, I.A. Cross, A.C. Kozen, J.R. Montague, E.C. Schundler, X. Wei, S.A. McGill, B.R. Landry, K.R. Maxcy-Pearson, M.M. Turnbull, C.P. Landee. *Phys. Rev.*, **B76**, 024439 (2007).
[45] V. Gadet, M. Verdaguer, V. Briois, A. Gleizes, J.P. Renard, P. Beauvillain, C. Chappert, T. Goto, K. Le Dang, P. Veillet. *Phys. Rev.*, **B44**, 705 (1991).